

# Space-resolved Resistive Measurement of Liquid Metal Wall Thickness<sup>a)</sup>

S.M.H. Mirhoseini<sup>b)</sup> and F.A. Volpe<sup>c)</sup>

Department of Applied Physics and Applied Mathematics, Columbia University, New York, NY 10027,  
USA

(Dated: 15 September 2022)

In a fusion reactor internally coated with liquid metal, it will be important to diagnose the thickness of the liquid at various locations in the vessel, as a function of time, and possibly respond to counteract undesired bulging or depletion. The electrical conductance between electrodes immersed in the liquid metal can be used as a simple proxy for the local thickness. Here a matrix of electrodes is shown to provide spatially resolved measurements of liquid metal thickness in the absence of plasma. First a theory is developed for  $m \times n$  electrodes, and then it is experimentally demonstrated for  $3 \times 1$  electrodes. The experiments were carried out with Galinstan, but are easily extended to Lithium or other liquid metals.

PACS numbers: 52.35.Py, 52.65.Kj, 61.25.Mv, 72.15.Cz

## I. INTRODUCTION

Liquid metals (LMs) are attractive low-recycling plasma-facing materials<sup>1–4</sup> that could protect the underlying solid walls of a fusion reactor from high heat and neutron fluxes<sup>5–7</sup>.

Lithium has been frequently used<sup>1–4</sup>, but Tin, Lithium-Tin alloys, Gallium, the molten salt LiBe and other materials are also being considered<sup>5–7</sup>. These materials introduce new diagnostic requirements compared with confinement devices featuring solid walls. For example, CDX-U and LTX were equipped with spectroscopic diagnostics in the visible and extreme ultraviolet, with special attention paid to neutral Lithium, Li II and Li III lines<sup>8,9</sup>.

An additional diagnostic requirement is posed by the very fact that these walls are liquid and thus can deform<sup>10</sup> under the effect of instabilities, turbulence, as a result of non-uniform force fields or currents from the plasma<sup>11–14</sup>. Deformations are undesired because they can cause the liquid metal to enter in contact with the plasma and thus contaminate it, cool it, limit it -in the sense of acting as a limiter-, possibly even disrupt it, or, on the contrary, expose the underlying solid wall to heat and neutrons. Therefore, deformations need to be monitored as a function of space and time, with resolutions of the order of a centimeter (in the poloidal and toroidal direction) and 10 ms<sup>14</sup>.

The sensitivity and precision in the radial direction, on the other hand, are dictated by the two lengthscales that need to be monitored and preserved. These are the distance between the LM surface and the last closed flux surface (typically few cm) and the LM thickness.

The thickness can range from sub-millimeter to meters, depending whether the LM is only used for its benign plasma-facing properties (low erosion, low recycling etc.) or is also meant to attenuate heat and neutrons. All things considered, millimeter precision is expected to suffice in most cases.

In a previous work<sup>14</sup> we had shown that, quite simply, and on the net of small corrections, the electrical conductance between two electrodes immersed in the LM scales linearly with the local LM thickness. Consequently, simple resistive measurements were used to infer the LM thickness in a single location and at a single time<sup>14</sup>.

Here, after briefly describing the experimental setup (Sec.II), we extend the measurements to multiple locations, requiring a matrix formalism (Sec.III), and discuss their integration with multiple actuators for thickness control (Sec.IV).

## II. EXPERIMENTAL SETUP

Here we recapitulate an earlier description of the setup<sup>14</sup> and report recent improvements.

The setup features a container filled for 5–25 mm with a low melting point (10°C) eutectic alloy of Gallium, Indium and Tin called Galinstan. This is about as good an electric conductor as Lithium (17% and 16% of copper, respectively).

Embedded in the container are  $3 \times 4$  copper electrodes of 2 mm diameter and various lengths, for the sake of comparison (1, 16 and 25 mm, with 25 mm yielding the best results<sup>14</sup>). Adjacent electrodes are spaced by 25 mm in one direction and 15 mm in the other.

The electrodes are connected to adjustable current-sources as well as to voltmeters referenced to ground. A shunt resistor is connected in series with the current-source, to measure the electrode current. As of recently, voltage and current signals are digitized at up to  $10^5$  KSa/s and digitally filtered from high-frequency noise (typically  $f < 500$  Hz). A LabView interface analyzes these data and returns the electrical resistance and LM

<sup>a)</sup>Contributed paper published as part of the Proceedings of the 19th Topical Conference on High-Temperature Plasma Diagnostics, Monterey, California, May, 2012.

<sup>b)</sup>shm2148@columbia.edu

<sup>c)</sup>fvolpe@columbia.edu

thickness between each pair of electrodes, in real time (typically every 10-100 ms).

### III. SPACE-RESOLVED MEASUREMENTS

#### A. Theory

Consider  $m \times n$  electrodes, evenly spaced in the  $x$  and  $y$  direction, at distances  $dx$  and  $dy$ , respectively, between adjacent electrodes. The electrodes are connected to individual power-supplies. These can inject or extract current in the LM system, in the  $z$  direction orthogonal to the  $xy$  plane. However, no charge is accumulated, and  $\nabla \cdot \mathbf{j} = 0$ . That is, Kirchhoff's law applies: the sum of all currents emitted or collected by an electrode is zero. The convention is adopted here that emitted currents are positive; collected currents are negative. In general, there are five such currents for each electrode: four in the  $xy$  plane, pointing at adjacent electrodes, and one in the  $z$  direction. Boundary or corner electrodes, on the other hand, only connect to three or two adjacent electrodes and one power supply.

Currents can obviously flow from or to *any* other electrode, not necessarily adjacent. Nonetheless, it is not necessary to model the system as a complicated network where all electrodes are directly connected to each other, forming a total of  $mn(mn - 1)/2$  connections. Instead, a Cartesian grid of  $(m - 1) \times (n - 1)$  resistors suffices. In this representation, each electrode is directly connected to only four adjacent electrodes via resistors, indicative of the LM thickness in between. Currents can flow from one electrode to another along several different routes on this Cartesian grid; the total resistance between two remote electrodes can be calculated by repeated application of simple sum rules for resistors in series or parallel. The total resistance between adjacent electrodes, on the other hand is, with good approximation, that of the very resistor that directly connects them.

Let us call  $I_{i,j}$  the current emitted by electrode  $i,j$  and directed at the power supply. Let  $V_{i,j}$  denote the potential of electrode  $i,j$  relative to some ground reference. The current emitted from electrode  $i,j$  to electrode  $i,j + 1$  will be proportional to the electric field  $E_y = (V_{i,j+1} - V_{i,j})/dy$ , to conductivity  $\sigma$ , and to the cross-sectional area  $h_{i,j+1/2}dx$ , where  $h_{i,j+1/2}$  is the LM height in the midpoint between the two electrodes. After similar considerations for the other electrodes in the stencil, Kirchhoff's law writes:

$$\begin{aligned} \frac{I_{ij}}{\sigma} = & \frac{V_{i,j} - V_{i,j+1}}{dy} h_{i,j+1/2} dx + \frac{V_{i,j} - V_{i,j-1}}{dy} h_{i,j-1/2} dx \\ & + \frac{V_{i,j} - V_{i+1,j}}{dx} h_{i+1/2,j} dy + \frac{V_{i,j} - V_{i-1,j}}{dx} h_{i-1/2,j} dy, \end{aligned} \quad (1)$$

except for boundaries and corners of the domain, where one or two terms drop from the right hand side. In this

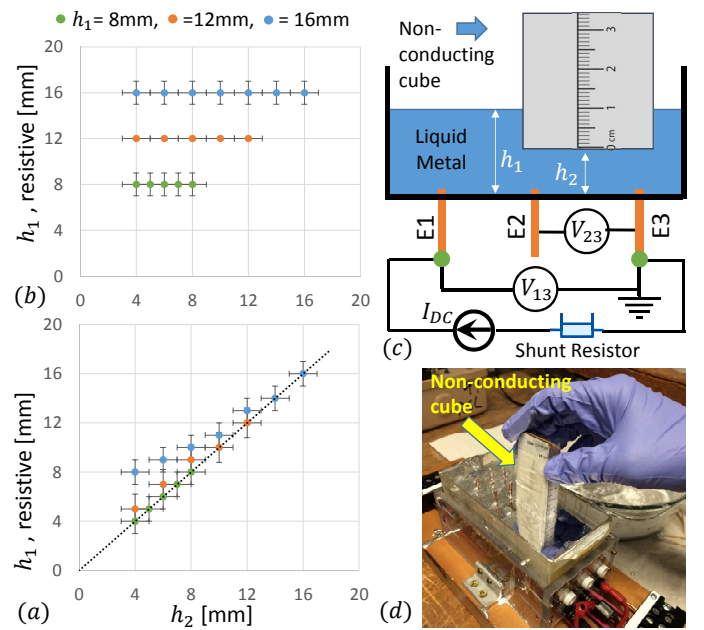


FIG. 1. Measurement results for a)  $h_1$  and b)  $h_2$  resistively measured versus  $h_2$  measured by a Teflon coated ruler, c) and d) scheme and the experimental setup of the space-resolved measurement test, respectively.

equation,  $\sigma$  is fixed by the material,  $dx$  and  $dy$  by the geometry, currents and voltages are measured, and the heights are the unknowns. Eq.1 describes a set of  $mn$  equations, but only  $(m - 1)(n - 1)$  of them are needed to solve for the  $(m - 1)(n - 1)$  unknowns. The problem can be cast in matrix form  $\mathbf{I} = \mathbf{A}\mathbf{h}$ . Here  $\mathbf{I}$  and  $\mathbf{h}$  are one-dimensional arrays containing  $(m - 1)(n - 1)$  values of currents and heights, respectively. The block-diagonal matrix  $\mathbf{A}$  is large, but features only five non-vanishing elements in each row (or four, or three, in rows corresponding to boundaries or corners), easily deduced from Eq.1. Ultimately we can solve for the LM heights by a simple matrix inversion,  $\mathbf{h} = \mathbf{A}^{-1}\mathbf{I}$ .

It should be noted that Ohm's law  $\mathbf{j} = \sigma\mathbf{E}$  was used in Eq.1, instead of the more general  $\mathbf{j} = \sigma(\mathbf{E} + \mathbf{v} \times \mathbf{B})$ . This is legitimate under the assumptions that: (1) the liquid wall is thin and not significantly bulging or depleting ( $v_z = 0$ ) and (2) there is no error field orthogonal to the wall ( $B_z = 0$ ). Under these assumptions,  $\mathbf{v} \times \mathbf{B}$  has no  $x$  nor  $y$  components, hence it cannot perturb the currents between electrodes. An alternative requirement is that (3) the flow is slow enough that the  $x$  and  $y$  components of  $\mathbf{v} \times \mathbf{B}$  are negligible compared with the corresponding components of  $\mathbf{E}$ . A realistic system violates these

assumptions, and Eq.1 needs to be generalized:

$$\begin{aligned} \frac{I_{ij}}{\sigma} = & \left[ \frac{V_{i,j} - V_{i,j+1}}{dy} + (v_x B_z - v_z B_x)_{i,j+\frac{1}{2}} \right] h_{i,j+\frac{1}{2}} dx \\ & + \left[ \frac{V_{i,j} - V_{i,j-1}}{dy} - (v_x B_z - v_z B_x)_{i,j-\frac{1}{2}} \right] h_{i,j-\frac{1}{2}} dx \\ & + \left[ \frac{V_{i,j} - V_{i+1,j}}{dx} + (v_z B_y - v_y B_z)_{i+\frac{1}{2},j} \right] h_{i+\frac{1}{2},j} dy \\ & + \left[ \frac{V_{i,j} - V_{i-1,j}}{dx} - (v_z B_y - v_y B_z)_{i-\frac{1}{2},j} \right] h_{i-\frac{1}{2},j} dy. \end{aligned} \quad (2)$$

This requires knowledge of the components of  $\mathbf{v}$  and  $\mathbf{B}$  in the midpoints between electrodes. Such knowledge could be provided by separate diagnostics, assumptions or calculations, or  $\mathbf{v}$  and  $\mathbf{B}$  might be reasonably fixed in the experiment. With this external input to matrix  $\mathbf{A}$ , the problem can be solved as a simple matrix inversion again,  $\mathbf{h} = \mathbf{A}^{-1} \mathbf{I}$ .

## B. Experiment

Three copper electrodes of 1 mm height in one row of the  $3 \times 4$  matrix have been used for space-resolved resistive measurement. The DC current generator is connected to the first and the last electrodes in the row (see Fig. 1). A LabView interface calculates the LM height between each pair of electrodes in real-time using the calculations in the previous section, with  $m = 3$  and  $n = 1$ . The following test has been accomplished to evaluate the accuracy of the developed theory. According to the Fig. 1, the LM depth between the electrodes E2 and E3 is changed by inserting a non-conducting cube in the space over and between these electrodes. Heights  $h_1$  and  $h_2$  are measured by the resistive sensor at the same time and are plotted in Fig. 1. From the results it is clear that the sensor is more accurate when measuring the LM thickness for lower  $h_1$  values. This is reasonable, since by increasing the LM height, the current between the short electrodes is not uniformly distributed, which decreases the accuracy of the applied theoretical method.

Another test was run with the same setup, where this time the LM thickness was varied by tilting the entire container, so that the average  $\langle h_1 \rangle$  increased and  $\langle h_2 \rangle$  decreased. The sensors correctly measured the  $\langle h_2 \rangle$  decrease, but underestimated the  $\langle h_1 \rangle$  increase. The reason for this is yet to be understood, but might be related to an approximation implicit in Eq.1, due to the discretization of the problem: the use of, say,  $h_{i,j+1/2}$  in the midpoint between electrodes  $i, j$  and  $i, j+1$  is equivalent to assuming the LM height to be locally uniform. This approximation was violated in the test on a tilted LM container, where the height varied linearly between one electrode and the next.

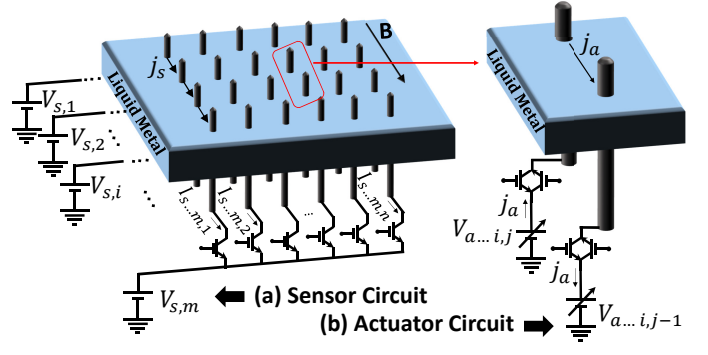


FIG. 2. a) Scheme of the Sensor circuit. IGBT switches control when the current is applied to the circuit and b) actuator circuit; anti-parallel IGBT bundle controls a bi-directional current path through each electrode. Subscripts  $s$  and  $a$  refer respectively to sensors and actuators, subscripts  $i$  and  $j$  refer to a specific electrode in a matrix of  $m \times n$  electrodes.

## IV. SENSOR AND ACTUATOR STRATEGY

The currents in Eqs.1,2 are applied for the purpose of measuring electrical conductance, proportional to height. Therefore, they can be small. Higher currents are necessary to apply stabilizing or gravity-defying  $\mathbf{j} \times \mathbf{B}$  forces, but, in principle, high  $\mathbf{j}$  could simultaneously sense thickness and serve as actuators.

However, an alternative strategy can also be envisioned, in which a square-waveform generator alternatively activates a sensor and an actuator circuit (Fig.2). Time-gaps without sensors or without actuators are tolerable, provided they are briefer than the timescale of interest (about 10 ms<sup>14</sup>).

In the sensor circuit (Fig.2a), insulated-gate bipolar transistors (IGBTs) act as switches injecting the currents  $I_{s...i,j}$ , for example from one boundary of the electrode matrix to the opposite one. Simultaneous voltage and current measurements through each electrode will provide the necessary data to evaluate the LM thickness at every electrode.

If the LM surface is perfectly even, electrical resistivity will be spatially uniform. If not, it will be necessary to use actuators to locally control the LM thickness. A simple criterion for a control system could consist of imposing uniform resistivity.

The anti-parallel arrangement of IGBT switches depicted in Fig.2b provides a bidirectional current path. Adequate compensating current density  $\mathbf{j}_a$ , calculated at the previous (sensing) stage, will be applied to the proper adjacent electrodes, as to locally exert a  $\mathbf{j}_a \times \mathbf{B}$  force, where needed to even out the LM surface. Similar to the sensor current, the actuator compensating current is pulsating. Therefore  $\mathbf{j}_a$  must be defined so that its time-average  $\langle \mathbf{j}_a \rangle$  equals the desired cw current.

## SUMMARY AND CONCLUSIONS

Liquid metal (LM) walls introduce new diagnostic needs. One of the most important observables will be the LM thickness. As shown earlier<sup>14</sup>, the electrical conductance between LM-immersed electrodes is a simple proxy for the local LM thickness. Here measurements of thickness were spatially resolved for the first time: first a theory was developed for  $m \times n$  electrodes, and then experimentally demonstrated for  $3 \times 1$  electrodes. The measurements were carried out with Galinstan in the absence of plasma, but are expected to succeed also with Lithium, whose conductivity is nearly identical.

Future work will be carried out in the presence of plasma. The diagnostic of thickness might require information from flowmeters and magnetics, due to com-

plications associated with error fields and rapid flows, theoretically discussed here. The integration with actuators controlling the LM thickness was also discussed.

- <sup>1</sup>R. Majeski *et al.*, *J. Nuclear Materials* **313**, 625 (2003)
- <sup>2</sup>R. Majeski *et al.*, *Nucl. Fusion* **45**, 519 (2005)
- <sup>3</sup>R. Kaita *et al.*, *Phys. Plasmas* **14**, 056111 (2007)
- <sup>4</sup>R. Majeski *et al.*, *Fusion Eng. Design* **85**, 1283 (2010)
- <sup>5</sup>R.W. Moir, *Nucl. Fusion* **37**, 557 (1997)
- <sup>6</sup>M.A. Abdou *et al.*, *Fusion Eng. Design* **54**, 181 (2001)
- <sup>7</sup>F.L. Tabares, *Plasma Phys. Control. Fusion* **58**, 014014 (2015)
- <sup>8</sup>R. Kaita *et al.*, *Rev. Sci. Instrum.* **72**, 915 (2001)
- <sup>9</sup>R. Majeski *et al.*, *Phys. Plasmas* **20**, 056103 (2013)
- <sup>10</sup>M. Narula *et al.*, *Fus. Eng. Design* **81**, 1543 (2006)
- <sup>11</sup>N.B. Morley, M.S. Tillack, *Magnetohydrodynamics* **2**, 69 (1993)
- <sup>12</sup>M.A. Jaworski *et al.*, *J. Nucl. Materials* **415**, S985 (2011)
- <sup>13</sup>H. Ait Abderrahmane, G.H. Vatistas, *Fusion Eng. Design* **83**, 661 (2008)
- <sup>14</sup>S.M.H. Mirhoseini, F.A. Volpe, *Plasma Phys. Control. Fusion*, submitted (2016), arXiv:1604.07473